Inorg. Chem. **2006**, *45*, 2758–2766

Influence of Solvent Composition on the Kinetics of Cyclooctene Epoxidation by Hydrogen Peroxide Catalyzed by Iron(III) [tetrakis(pentafluorophenyl)] Porphyrin Chloride [(F_{20}TPP)FeCl]

Ned A. Stephenson and Alexis T. Bell*

Chemical Sciences Division, Lawrence Berkeley Laboratory and Department of Chemical Engineering, University of California, Berkeley, California 94720-1462

Received December 22, 2005

The epoxidation of cyclooctene catalyzed by iron(III) [tetrakis(pentafluorophenyl)] porphyrin chloride [(F_{20}TPP)FeCl] was investigated in alcohol/acetonitrile solutions in order to determine the effects of the alcohol composition on the reaction kinetics. It was observed that alcohol composition affects both the observed rate of hydrogen peroxide consumption (the limiting reagent) and the selectivity of hydrogen peroxide utilization to form cyclooctene epoxide. The catalytically active species are formed only in alcohol-containing solvents as a consequence of (F_{20}TPP)FeCl dissociation into [(F_{20}TPP)Fe(ROH)]$^+$ cations and Cl^- anions. The observed reaction kinetics are analyzed in terms of a proposed mechanism for the epoxidation of the olefin and the decomposition of H_2O_2. The first step in this scheme is the reversible coordination of H_2O_2 to [(F_{20}TPP)Fe(ROH)]$^+$. The O–O bond of the coordinated H_2O_2 then undergoes either homolytic or heterolytic cleavage. The rate of homolytic cleavage is found to be independent of alcohol composition, whereas the rate of heterolytic cleavage increases with alcohol acidity. Heterolytic cleavage is envisioned to form iron(IV) π-radical cations, whereas homolytic cleavage forms iron(IV) hydroxo cations. The iron(IV) radical cations are active for olefin epoxidation, whereas the iron(IV) cations catalyze the decomposition of H_2O_2. Reaction of iron(IV) π-radical cations with H_2O_2 to form iron(IV) hydroxo cations is also included in the mechanism, a process that is favored by alcohols with a high charge density on the O atoms. The proposed mechanism describes successfully the effects of H_2O_2, cyclooctene, and porphyrin concentrations, as well as the effects of alcohol concentration.

Introduction

Iron(III) porphyrins have been the subject of considerable interest, since they are good models of heme-type catalysts found in nature.[1−3] A large part of this effort has been devoted to understanding the factors affecting the activity and selectivity of porphyrins for the epoxidation of olefins and the hydroxylation of various hydrocarbons. Particular attention has focused on iron(III) porphyrins with electron-withdrawing groups attached to the periphery of the porphyrin ring because they are highly active and relatively stable to oxidative degradation.[4−6] One of the most studied of this class of iron porphyrins is iron(III) [tetrakis-(pentafluorophenyl)] porphyrin [(F_{20}TPP)Fe].[5−29]

Since (F_{20}TPP)Fe^{III} is a cation, it is must be charge-compensated by an anion, X. Nam and co-workers have[6] reported that the catalytic activity of the porphyrin is affected

* To whom correspondence should be addressed. E-mail: bell@cchem.berkeley.edu.

(1) Sheldon, R. A. *Metalloporphyrins in Catalytic Oxidations*; Marcel Dekker: New York, 1994.
(2) Montanari, F.; Casella, L. *Metalloporphyrins Catalyzed Oxidations*; Kluwer Academic Publishers: Boston, 1994.
(3) Meunier, B. *Biomimetic Oxidations Catalyzed by Transition Metal Complexes*; Imperial College Press: London, 1999.
(4) Gross, Z.; Simkhovich, L. *Tetrahedron Lett.* **1998**, *39*, 8171−8174.
(5) Grinstaff, M. W.; Hill, M. G.; Labinger, J. A. *Science*. **1994**, *264*, 1311−1313.
(6) Birnbaum, E. R.; Grinstaff, M. W.; Labinger, J. A.; Bercaw, J. E.; Gray, H. B. *J. Mol. Catal. A: Chem*. **1995**, *104*, L119−L122.
(7) Lee, K. A.; Nam, W. *Bull. Kor. Chem. Soc.* **1996**, *17*, 669−671.
(8) Lee, K. A.; Nam, W. *J. Am. Chem. Soc.* **1997**, *119*, 1916−1922.
(9) Nam, W.; Lee, H. J.; Oh, S. Y.; Kim, C.; Jang, H. G. *J. Inorg. Biochem.* **2000**, *80*, 219−225.
(10) Nam, W.; Lim, M. H.; Lee, H. J.; Kim, C. *J. Am. Chem. Soc.* **2000**, *122*, 6641−6647.
(11) Nam, W.; Lim, M. H.; Moon, S. K.; Kim, C. *J. Am. Chem. Soc.* **2000**, *122*, 10805−10809.
(12) Nam, W.; Lim, M. H.; Oh, S. Y.; Lee, J. H.; Woo, S. K.; Kim, C. *Angew. Chem., Int. Ed.* **2000**, *39*, 3646−3649.
(13) Manso, C. M. C. P.; Neri, C. R.; Vidoto, E. A.; Sacco, H. C.; Ciuffi, K. J.; Iwamoto, L. S.; Iamamoto, Y.; Nascimento, O. R.; Serra, O. A. *J. Inorg. Biochem.* **1999**, *73*, 85−92.

10.1021/ic0521776 CCC: $33.50
Published on Web 02/11/2006

by the composition of the anion and the solvent in which the porphyrin is dissolved. If, for example, $X = Cl^-$ or CH_3O^-, then the porphyrin is catalytically inactive in an aprotic solvent but becomes active if $X = NO_3^-$, SbF_6^-, $CF_3SO_3^-$, or ClO_4^-.[12] The use of a protic solvent or a mixture of protic and aprotic solvents can result in the activation of porphyrins that are inactive in an aprotic solvent. Thus, for example, (F_{20}TPP)FeCl has been reported to be inactive for olefin epoxidation when dissolved in acetonitrile but becomes active when methanol or another alcohol is added to the aprotic solvent.[17,19,28] We have demonstrated recently that (F_{20}TPP)FeX must first dissociate in order to become active.[29] This process requires that both the cation and anion are solvated and involves coordination of the solvent to the $[(F_{20}TPP)Fe]^+$ cation. Thus, in the case of (F_{20}TPP)FeCl dissolved in CH_3OH or a mixture of CH_3CN and CH_3OH, the active form of the porphyrin is $[(F_{20}TPP)Fe(CH_3OH)]^+$.

The mechanism by which iron(III) porphyrins catalyze the epoxidation of olefins has also been the subject of many studies.[1−3] Unfortunately, much of this literature describes work done with different porphyrins, solvents, olefins, and oxidants (e.g., H_2O_2, ROOH, PhIO, mCPBA), making it difficult to ascertain unambiguously the structure of the active species and the reaction pathways via which reactants are formed and oxidant is consumed. A further complication has been the scarcity of rate data for both the formation of product(s) and the consumption of oxidant, with the result that it is often impossible to establish whether a proposed mechanism is, or is not, consistent with the measured reaction rates. The situation is considerably better for the case of cyclooctene epoxidation by H_2O_2 catalyzed by (F_{20}TPP)Fe, since only one product, cyclooctene oxide, is produced.[10,22] The consensus view in this case is that epoxidation begins with the equilibrium coordination of H_2O_2 to (F_{20}TPP)Fe. The O−O bond of the peroxide can then cleave either homolytically or heterolytically to produce either an iron(IV) cation or an iron(IV) π-radical cation, respectively. The first of these species is involved in the decomposition of H_2O_2, whereas the second is responsible for the epoxidation of cyclooctene. We have recently shown that a mechanism containing all of these elements, as well as a reaction for the conversion of iron(IV) π-radical cations to iron(IV) cations, provides a very good description of the kinetics of cyclooctene epoxidation by H_2O_2 catalyzed by (F_{20}TPP)FeCl dissolved in a mixture of methanol and acetonitrile.[28] Equilibrium constants and rate coefficients were determined for each of the elementary processes involved in the epoxidation mechanism. It was also demonstrated that the same rate parameters can be used to describe the kinetics of H_2O_2 consumption in the presence and absence of the olefin. A further finding of this work was that the presence of methanol facilitates the heterolytic cleavage of the O−O bond of H_2O_2, as originally suggested by Traylor and coworkers.[30]

The objective of the present study was to determine the effects of alcohol composition on the kinetics of cyclooctene epoxidation and the selectivity of H_2O_2 consumption toward olefin epoxidation versus decomposition to water and oxygen. (F_{20}TPP)FeCl was used as the catalyst for all of this work, and the alcohols used included methanol, ethanol, *n*-propanol, *i*-propanol, *n*-butanol, and *t*-butanol. The formation of cyclooctene oxide was determined by gas chromatography, and the consumption of H_2O_2 was determined by ^{1}H NMR.

Experimental Section

Reagents. Non-UV grade acetonitrile (99.99%), methanol (99.98%), ACS grade chloroform (99.8%), hydrogen peroxide (30%), *t*-butanol (99.4%), and *i*-propanol (99.99%) were obtained from EMD Chemicals. (F_{20}TPP)FeCl, dodecane (99+%), *n*-propanol (99.8+%), and *n*-butanol (99.9%) were obtained from Sigma Aldrich. *Cis*-cyclooctene (95%) was obtained from Alfa-Aesar. Deuterium oxide (99.8%) was obtained from Cambridge Isotope Laboratories, Inc.

Reactions. All reactions were carried out in 5 mL reaction vials at room temperature (298 K). The reaction mixture was stirred magnetically with spin-vane stir bars throughout the reaction. The total reaction volume was 3.35 mL for all reactions. The solvent consisted of a mixture of alcohol and acetonitrile, 6.2 M in alcohol unless otherwise stated. Ten microliters of dodecane was used as an internal standard. The cyclooctene and hydrogen peroxide concentrations were varied depending upon the experiment. Hydrogen peroxide was added to the reactor vial using a microsyringe after all other components had been added to the vial. Time zero for a reaction was defined as the time at which the hydrogen peroxide was added to the vial.

Analysis of Reaction Products. The presence of cyclooctene epoxide in the reaction products was detected via gas chromatography, and its concentration was determined by comparison of the peak area of epoxide to the peak area of the internal standard. An HP6890 series gas chromatograph fitted with an Agilent DB Wax (30 m × 0.32 mm × 0.5 μm) capillary column, and an FID detector was used for the analysis. Since each chromatographic analysis

(14) Lim, M. H.; Jin, S. W.; Lee, Y. J.; Jhon, G. J.; Nam, W.; Kim, C. *Bull. Kor. Chem. Soc.* **2001**, *22*, 93−96.
(15) Nam, W.; Jin, S. W.; Lim, M. H.; Ryu, J. Y.; Kim, C. *Inorg. Chem.* **2002**, *41*, 3647−3652.
(16) Nam, W.; Park, S. E.; Lim, I. K.; Hong, J.; Kim, J. *J. Am. Chem. Soc.* **2003**, *125*, 14674−14675.
(17) Nam, W.; Oh, S. Y.; Sun, Y. J.; Kim, J.; Kim, W. K.; Woo, S. K.; Shin, W. *J. Org. Chem.* **2003**, *68*, 7903−7906.
(18) Traylor, T. G.; Tsuchiya, S.; Byun, Y. S.; Kim, C. *J. Am. Chem. Soc.* **1993**, *115*, 2775−2781.
(19) Traylor, T. G.; Kim, C.; Richards, J. L.; Xu, F.; Perrin, C. L. *J. Am. Chem. Soc.* **1995**, *117*, 3468−3474.
(20) Collman, J. P.; Chien, A. S.; Eberspacher, T. A.; Brauman, J. I. *J. Am. Chem. Soc.* **2000**, *122*, 11098−11100.
(21) Cunningham, I. D.; Danks, T. N.; O'Connel, K. T. A.; Scott, P. W. *J. Chem. Soc., Perkin Trans. 2* **1999**, 2133−2139.
(22) Cunningham, I. D.; Danks, T. N.; Hay, J. N.; Hamerton, I.; Gunathilagan, S. *Tetrahedron* **2001**, *57*, 6847−6853.
(23) Cunningham, I. D.; Danks, T. N.; Hay, J. N.; Hamerton, I.; Gunathilagan, S.; Janczak, C. *J. Mol. Catal. A.: Chem.* **2002**, *185*, 25−31.
(24) Fujii, H. *Chem. Lett.* **1994**, 1491−1494.
(25) Fujii, H. *Coord. Chem. Rev.* **2002**, *226*, 51−60.
(26) Wadhwani, P.; Mukherjee, M.; Bandyopadhyay, D. *J. Am. Chem. Soc.* **2001**, *123*, 12430−12431.
(27) Selke, M.; Valentine, J. S. *J. Am. Chem. Soc.* **1998**, *120*, 2652−2653.
(28) Stephenson, N. A.; Bell, A. T. *J. Am. Chem. Soc.* **2005**, *127*, 8635−8643.
(29) Stephenson, N. A.; Bell, A. T. *Inorg. Chem.* **2006**, submitted for publication.
(30) Traylor, T. G.; Xu, F. *J. Am. Chem. Soc.* **1990**, *112*, 178−186.

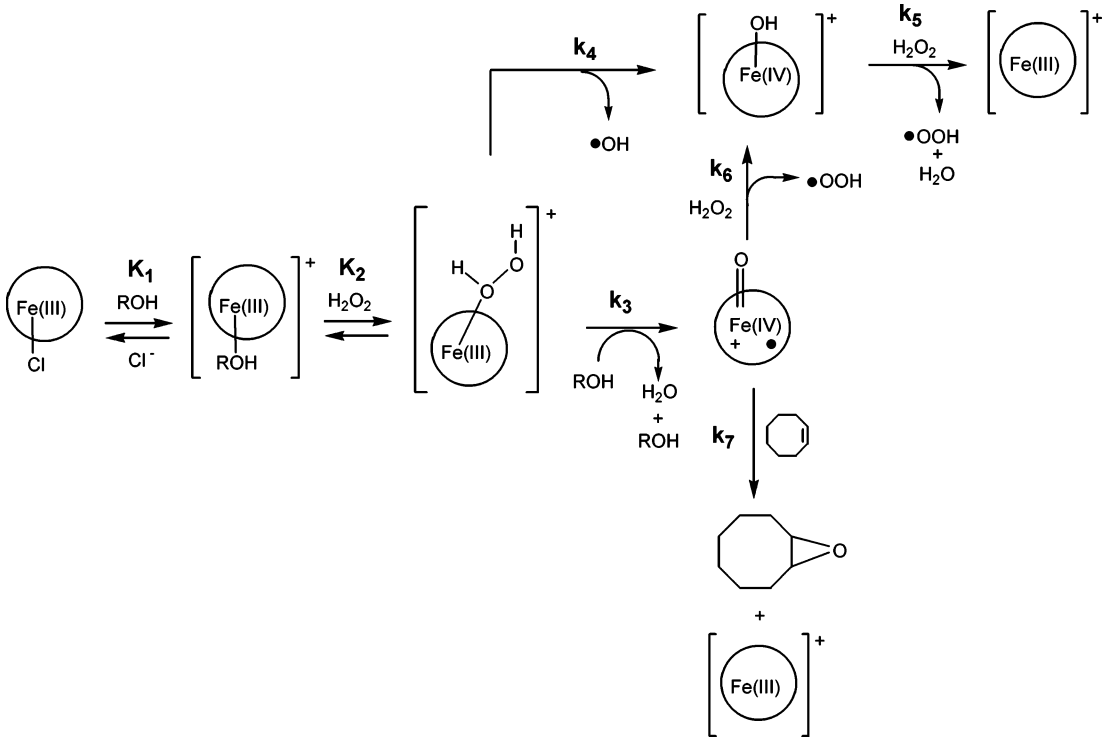

Figure 1. Mechanism for the epoxidation of cyclooctene and the decomposition of hydrogen peroxide via (F_{20}TPP)Fe.

required 15 min, multiple reactions were used to collect product concentration data as a function of time. Data were obtained in triplicate to ensure precision. The repeatability of the data was ±2%. The accuracy of measuring the epoxide concentration via gas chromatography was ±1% based on analysis of a calibrated standard.

The hydrogen peroxide concentration was measured in situ as a function of time via ^{1}H NMR using a 400 MHz Bruker VMX spectrometer. For these experiments, a concentrated catalyst solution was injected into the NMR reaction tube containing all other components immediately prior to the initiation of data collection. A data point was collected either every 32 or 64 s by averaging the data from 4 or 8 scans. The data point collection interval was determined by the rate of reaction. Quantification of hydrogen peroxide was done by integrating the area of the hydrogen peroxide peak, located at approximately 10.3 ppm, and comparing it to the area of the peak for the internal standard, chloroform. A more detailed description of the NMR technique can be found elsewhere.[28,31]

UV−visible spectroscopy was used to characterize the axial coordination, oxidation state, and degradation of the porphyrin. Absorbance experiments were conducted using a Varian Cary 400 Bio UV−visible spectrometer. Porphyrin degradation was quantified by integrating the area under the peaks between 280 and 700 nm. An extinction coefficient was determined from standardized samples. The systematic error associated with UV−visible scans was negligible.

Axial coordination to the porphyrin was characterized via paramagnetic NMR, using a 400 MHz Bruker VMX spectrometer. As reported previously, in the presence of an alcohol, (F_{20}TPP)-FeCl dissociates the chloride ligand to produce [(F_{20}TPP)Fe(ROH)]$^+$ cations and Cl$^-$ anions.[29] This process is evidenced by an upfield shift of the β-pyrrole proton peak.

(31) Stephenson, N. A.; Bell, A. T. *Anal. Bioanal. Chem.* **2005**, *381*, 1289−1293.

Analysis of Reaction Kinetics

The kinetics of cyclooctene epoxidation and hydrogen peroxide consumption are described on the basis of the mechanism shown in Figure 1. This scheme is very similar to that used to analyze the epoxidation of cyclooctene by hydrogen peroxide catalyzed by (F_{20}TPP)FeCl in methanol/acetonitrile solutions.[28] The first step, Reaction 1, is the dissociation of (F_{20}TPP)FeCl into [(F_{20}TPP)Fe(ROH)]$^+$ cations and Cl$^-$ anions. As demonstrated for the case of methanol, the cation is stabilized by the coordination of a molecule of methanol, as well as general solvation by methanol, and the chloride anion is stabilized by methanol solvation.[29] (Note: for clarity, the alcohol ligand is not shown after Reaction 2.) Hydrogen peroxide then coordinates reversibly in Reaction 2 to the [(F_{20}TPP)Fe(ROH)]$^+$ cation. The O−O bond of the coordinated H_2O_2 can undergo either heterolytic or homolytic cleavage. The first of these processes, Reaction 3, is facilitated by interaction of a molecule of alcohol with the coordinated H_2O_2, as illustrated in detail in Figure 2. Since the alcohol is somewhat acidic, the proton on ROH can be transferred to the OH group of H_2O_2 farthest from the Fe(III) cation to produce water, whereas the alkoxide group of ROH picks up the H atom of the OH group of H_2O_2 attached to Fe(III) and reforms the alcohol. Thus, the alcohol plays the role of a proton-transfer agent. The product of heterolytic cleavage of the O−O bond is an iron(IV) π-cation radical. Homolytic cleavage of the O−O bond of coordinated H_2O_2 is shown as producing an HO$^\bullet$ radical and an iron(IV) hydroxo cation. In our previous work,[28] we have shown the latter species to be an iron(IV) oxo species, but a recent theoretical study by Silaghi-Dumitrescu indicates that the product of homolytic cleavage is more likely a

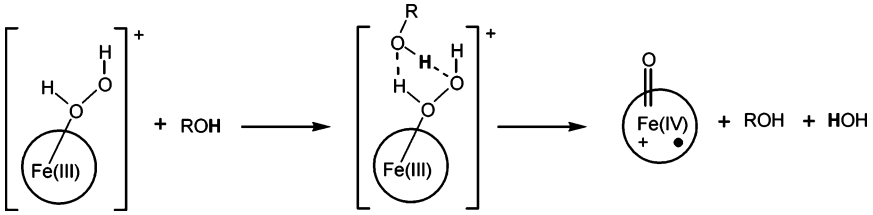

Figure 2. Details of the elementary process involved in Reaction 3 (see Figure 1).

Table 1. Summary of Results and Kinetic Parameters Based on the Presented Mechanism Applied to Different Alcohol-Based Solvent Systems with a 6.2 M Alcohol Concentration[a]

variable	methanol	ethanol	*n*-propanol	*n*-butanol	*i*-propanol
pK_a	15.3	15.9	16.1	16.1	17.1
porphyrin degradation with olefin	10%	10%	18%	24%	30%
porphyrin degradation without olefin	21%	23%	44%	53%	100%
epoxide yield, wrt H_2O_2	88%	86%	79%	79%	74%
[Fe − ROH] (μM)	46	49	59	57	44
k_{obs} (min^{-1})	0.25	0.24	0.15	0.14	0.09
K_1 from GC	1.2×10^{-5}	1.5×10^{-5}	3.5×10^{-5}	3.0×10^{-5}	1.0×10^{-5}
K_1 from NMR	1.0×10^{-5}	1.5×10^{-5}	3.3×10^{-5}	2.8×10^{-5}	0.9×10^{-5}
k_3K_2 ($M^{-1}\cdot s^{-1}$) (from GC data)	13	11	5.3	5.2	4.2
k_4K_2 (s^{-1}) (from GC data)	5.5	5.7	4.4	4.3	4.6
k_3/k_4 (M-1) (from GC data)	2.38	1.99	1.22	1.22	0.92
k_3K_2 ($M^{-1}\cdot s^{-1}$) (from GC and NMR data)	12	11	5.3	5.0	4.0
k_4K_2 (s^{-1}) (from GC and NMR data)	5.0	5.7	4.4	4.1	4.4
k_3/k_4 (M^{-1}) (from GC and NMR data)	2.38	1.99	1.22	1.23	0.92
k_5 ($M^{-1}\cdot s^{-1}$)	225	225	225	225	225
k_6/k_7	0.30	0.45	0.60	0.65	0.95

[a] Error bars for yields are ±2%, and error bars for rate constants are ±10%

hydroxo species rather than an oxo species.[37] The iron(IV) π-radical cation, which is the product of Reaction 3, can participate in two reactions. The first process involves reaction with H_2O_2, Reaction 6, to produce a HOO• radical and an iron(IV) hydroxo cation, and the second process is the epoxidation of cyclooctene, Reaction 7. The iron(IV) hydroxo cations produced in Reactions 4 and 6 can react with H_2O_2 in Reaction 5 to produce HOO• radicals, H_2O, and iron(III) cations. The latter cations are also produced as products of Reaction 7 and are the same as the original species involved in Reaction 1. The only additional difference between the mechanism shown in Figure 1 and that presented originally[28] is that a molecule of alcohol is not involved in Reaction 5.

The changes to the original version of the reaction mechanism do not affect the ability of the model to describe all features of the observed reaction kinetics, as will be shown in the next section. We note that there are some differences in the values reported in our previous work and the values shown in Table 1; this is due to the above-mentioned changes to the mechanism which resulted in some kinetic parameters being multiplied or divided by the experimental alcohol concentration. The values of K_1, k_3K_2, k_4K_2, and k_6/k_7 were obtained by fitting the kinetics predicted by the mechanism appearing in Figure 1 to the experimental data obtained in this study. Similar fits of the model to the data were obtained for five alcohol/acetonitrile solutions and for experiments in which the porphyrin concentration was varied for a constant alcohol/acetonitrile concentration or the alcohol concentration was varied for a fixed porphyrin concentration. The value of k_5 was taken to be the same as that observed for experiments conducted in methanol/acetonitrile solutions and not dependent on the alcohol composition.

Results and Discussion

The effects of alcohol composition on various properties and parameters are summarized in Table 1. The reported pK_a values are taken from ref 33. The percent of porphyrin that was degraded during reaction is reported for experiments performed with and without olefin present and is based on UV−visible measurements made at the beginning and end of a reaction. The latter point was determined in most cases by the complete consumption of hydrogen peroxide, the limiting reagent. However, when the decomposition of hydrogen peroxide was studied in an *i*-propanol/acetonitrile mixture, the complete degradation of the porphyrin occurred prior to the complete consumption of hydrogen peroxide. The epoxide yield is defined by the following relationship.[28]

$$Y_\infty = \frac{[C_8 - O]_\infty}{[H_2O_2]_0} \times 100\% \cong \frac{k_3[ROH]}{k_3[ROH] + 2k_4} \times 100\% \quad (1)$$

where $[C_8 - O]_\infty$ is the concentration of cyclooctene epoxide present in solution at the end of reaction, i.e., when all of the H_2O_2 has been consumed, and $[H_2O_2]_0$ is the concentra-

(32) Silaghi-Dumitrescu, R. *J. Biol. Inorg. Chem.* **2004**, *9*, 471−476.
(33) Howard, P. H.; Meylan, W. M. *Handbook of Physical Properties of Organic Chemicals*; CRC Lewis Publishers: Boca Raton, FL, 1989.
(34) Hashimoto, S.; Mizutani, Y.; Tatsuno, Y.; Kitagawa, T. *J. Am. Chem. Soc.* **1999**, *113*, 6542−6549.
(35) Fidler, V.; Ogura, T.; Sato, S.; Aoyagi, K.; Kitagawa, T. *Bull. Chem. Soc. Jpn.* **1991**, *64*, 2315−2322.
(36) Traylor, T. G.; Kim, C.; Fann, W. P.; Perrin, C. L. *Tetrahedron.* **1998**, *54*, 7977−7986.
(37) Traylor, T. G.; Ciccone, J. P. *J. Am. Chem. Soc.* **1989**, *111*, 8413−8420.

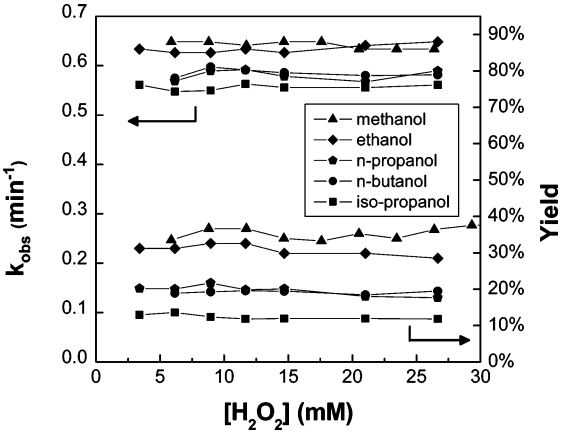

Figure 3. Effects of H_2O_2 concentration on the observed reaction rate coefficient for the consumption of H_2O_2 and the yield of cyclooctene oxide based on H_2O_2 consumption. The upper set of data points is the yield, while the lower set of data points is the observed rate coefficient.

tion of H_2O_2 at the start of the reaction. Y_∞ represents the yield at the end of the reaction, when all of the H_2O_2 has been consumed; however, as shown in ref 28, the yield is independent of reaction time provided that the initial concentration of cyclooctene is in large excess of the initial concentration of hydrogen peroxide. This requirement was always satisfied, since the ratio of hydrogen peroxide to cyclooctene was 50 for all of the case listed in Table 1. K_1 was determined by two independent techniques[28,29] and is reported in both cases for an alcohol concentration of 6.2 M. The concentration of $[(F_{20}TPP)Fe(ROH)]^+$ was determined from eq 2, using the listed value of K_1. The total concentration of porphyrin, $[Fe - Cl]_0$, used for these calculations was 74.7 μM.

$$[Fe - ROH] = \frac{-K_1[ROH] + \sqrt{(K_1[ROH])^2 + 4K_1[ROH][Fe - Cl]_0}}{2} \quad (2)$$

The observed first-order rate constant for hydrogen peroxide consumption, k_{obs}, is defined according to eq 3.[28] The value of k_{obs} was determined from the initial rate of formation of cyclooctene oxide and the value of Y_∞ (see eq 1). The value of k_3K_2 was then obtained from eq 3.

$$k_{obs} = \frac{k_3K_2[Fe - ROH][ROH]}{Y_\infty} \quad (3)$$

Here $[Fe - ROH]$ represents the concentration of $[(F_{20}TPP)Fe(ROH)]^+$ cations. Once k_3K_2 is known, then k_3/k_4 and k_4K_2 can be determined from the measured value of Y_∞ using the second part of eq 1. The ratio of the rate constants for Reactions 6 and 7, k_6/k_7, was determined by fitting the proposed reaction kinetics to the measured epoxide yield obtained as a function of the initial concentration of cyclooctene for a fixed concentration of hydrogen peroxide.[28]

Observed Rate Constant, k_{obs}. Equations 1 and 3 predict that both Y_∞ and k_{obs} should be independent of the concentration of H_2O_2. Figure 3 shows this to be the case for each of the alcohols investigated, which indicates that the mechanism proposed to interpret the rates of cyclooctene epoxidation and hydrogen peroxide consumption for $(F_{20}TPP)FeCl$ dissolved in methanol/acetonitrile solutions is equally valid for reactions occurring in other alcohol/acetonitrile solutions.

As seen in Table 1, the value of k_{obs} depends on the composition of the alcohol in the solvent and decreases in the order $CH_3OH \approx C_2H_5OH > n\text{-}C_3H_7OH \approx n\text{-}C_4H_9OH > i\text{-}C_3H_7OH$. The value of Y_∞ follows a similar pattern. Therefore, it is apparent that alcohol composition affects both the rate of H_2O_2 consumption and the fraction of the H_2O_2 that is utilized for epoxidation. Since both k_{obs} and Y_∞ are functions of several rate and equilibrium parameters, it is necessary to examine how alcohol composition affects these parameters in order to appreciate the effects of alcohol composition on the observed overall kinetics.

Formation of the Active Species, $[(F_{20}TPP)Fe(ROH)]^+$. It is evident from eq 3 that k_{obs} is proportional to the concentration of $[(F_{20}TPP)Fe(ROH)]^+$, and as shown in eq 2 above, the concentration of this species depends on the value of K_1, all other factors being the same. Table 1 shows that the value of K_1 increases with increasing chain length for straight-chained alcohols containing 1−4 carbon atoms. This trend is attributed to stronger binding of longer-chained normal alcohols to $[(F_{20}TPP)Fe]^+$ cations as a consequence of the increasing negative charge on the O atom of the alcohol as the length of the alkyl group increases. As discussed previously, the dissociation of $(F_{20}TPP)FeCl$ into cations and anions, which occurs in alcohol-containing solvents, depends on both solvation of the Cl^- anion and coordination of a molecule of alcohol to the $[(F_{20}TPP)Fe]^+$ cation.[29] The lower value of K_1 for *i*-propanol relative to *n*-propanol is attributed to steric effects, since otherwise, one would expect *i*-propanol to be more effective than *n*-propanol in stabilizing $[(F_{20}TPP)Fe]^+$ cations. Consistent with this reasoning, we observed that *t*-butanol was completely ineffective in promoting the dissociation of $(F_{20}TPP)FeCl$. The failure of *t*-butanol to coordinate axially to porphyrins has been noted previously and has been ascribed to steric hindrance between the methyl groups of the alcohol and the pyrrole nitrogen atoms.[34,35] It is important to observe that, while alcohol chain length affects the value of K_1, the concentration of $[(F_{20}TPP)Fe(ROH)]^+$ cations increase to a much smaller degree, as can be see from Table 1 (Note: all values of K_1 are reported for an alcohol concentration of 6.2 M). Thus, the noticeable effect of alcohol composition on the value of k_{obs} must be attributed to factors other than changes in the concentration of $[(F_{20}TPP)Fe(ROH)]^+$ cations. In particular, reference to eqs 1 and 3 shows that k_{obs} depends on the values of k_3K_2 and k_3/k_4. Therefore, the influence of alcohol composition on these parameters is examined next.

Effect of Alcohol on Heterolytic versus Homolytic Cleavage of the O−O Bond in Coordinated H_2O_2. Table 1 shows that the value of k_3K_2 is strongly affected by alcohol composition, decreasing in the order $CH_3OH > C_2H_5OH > n\text{-}C_3H_7OH \approx n\text{-}C_4H_9OH > i\text{-}C_3H_7OH$. By contrast, the value of k_4K_2 changes to only a limited extent with alcohol composition. Since Reaction 4 does not depend explicitly

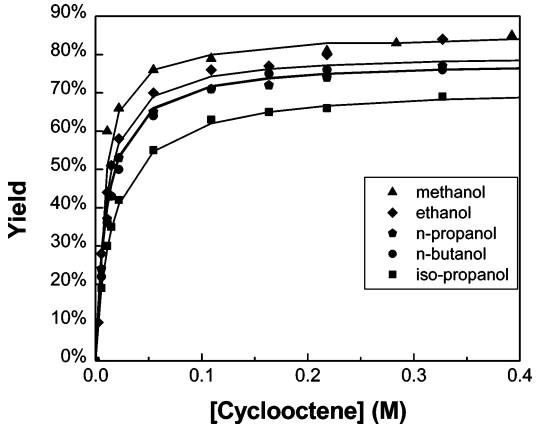

Figure 4. Effect of cyclooctene concentration on the final yield of cyclooctene epoxide. The solid lines represent the yield predicted on the basis of the mechanism shown in Figure 1.

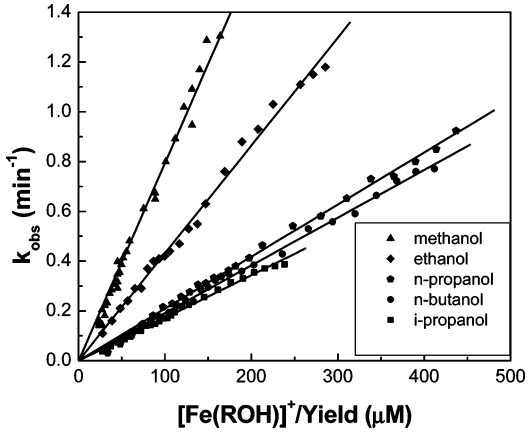

Figure 5. Relationship between k_{obs} and [Fe − ROH]/Y_∞ when the total porphyrin concentration is varied while the alcohol concentration is kept constant at 6.2 M.

on the composition of the alcohol, the near constancy of the values of k_4K_2 with alcohol composition suggests that the value of K_2, the equilibrium constant for the coordination of H_2O_2 by $[(F_{20}TPP)Fe(ROH)]^+$ cations, is also not much affected by alcohol composition. It then follows that the observed trend in the magnitude of k_3K_2 with alcohol composition is due predominantly to changes in the value of k_3. Table 1 shows that the decrease in the value of k_3/k_4, as one moves from methanol to *i*-propanol, parallels the decreasing acidity of the alcohols, as evidenced by their increasing pK_a. This trend indicates that alcohol acidity is an important factor in determining the rate coefficient for Reaction 3, the heterolytic cleavage of the O−O bond of H_2O_2. As seen in Figure 2, this process is envisioned to occur in a concerted fashion via the interaction of ROH with $[(F_{20}TPP)Fe(H_2O_2)(ROH)]^+$ cations. The net result of this reaction is the formation of the Fe(IV) π-radical cation and H_2O. The molecule of alcohol involved in the reaction is released and, hence, serves only as a catalyst. This conclusion is consistent with the idea of Traylor and co-workers,[30,36,37] who proposed that the heterolytic cleavage of the O−O bond of H_2O_2 coordinated to porphyrins occurs via a general acid-catalyzed process.

Competition for the Fe(IV) π-Radical Cation. While the relative rates of Reactions 6 and 7 can also affect the yield of epoxide, Reaction 6 occurs at a much lower rate than Reaction 7 when the initial concentration of olefin is strongly in excess of the concentration of hydrogen peroxide. This point is clearly seen in Figure 4. Thus, for the case where the initial concentration of H_2O_2 is 14.7 mM and the initial concentration of cyclooctene is 0.72 M, the yield of epoxide is dictated solely by the ratio of k_3/k_4 for a fixed alcohol concentration. However, as the concentration of cyclooctene is decreased, the yield decreases and eventually goes to zero. The curves shown in Figure 4 for each alcohol were obtained by adjusting the value of k_6/k_7, keeping the value of all other rate parameters constant. As can be seen in Table 1, the value of k_6/k_7 increases in the order CH_3OH < C_2H_5OH < *n*-C_3H_7OH ≈ C_4H_9OH < *i*-C_3H_7OH. Here again, this trend parallels the increase in pK_a values, suggesting that epoxidation of cyclooctene (Reaction 7) becomes more favorable relative to the conversion of the Fe(IV) radical cation to the Fe(IV) hydroxo cation (Reaction 6) as the electron density on the O atom of the coordinated alcohol decreases. This pattern is consistent with the observations of Nam and co-workers, who have shown that high-valent iron oxo intermediates with electron-deficient porphyrins react rapidly with olefins.[38] We suggest that that these observations indicate that, as the electron density on the porphyrin ring increases, the Fe(IV) radical cation becomes less effective in promoting olefin epoxidation and becomes susceptible to reaction with hydrogen peroxide to produce Fe(IV) hydroxo cations.

Effects of Porphyrin and Alcohol Concentration on k_{obs}. In the experiments discussed to this point, the initial porphyrin concentration and the concentration of alcohol in the solvent were kept constant. Therefore, it is of interest to establish whether the mechanism proposed in Figure 1 describes k_{obs} as these variables are changed. Reference to eqs 1−3 indicates that k_{obs} should be proportional to [Fe − ROH]/Y_∞ (eq 2), with the value of [Fe − ROH] given by eq 3 and the value of Y_∞ given by eq 1. Variation of the porphyrin concentration at a fixed alcohol concentration should have no effect on Y_∞, and hence, k_{obs} should change only as a consequence of changes in [Fe − ROH]. Figure 5 shows that in all cases k_{obs} obeys eq 2 when the initial porphyrin concentration is varied from 30 to 900 μM. The slope of each straight line is equal to the product of k_3K_2 and the alcohol concentration, and the values obtained from the slopes are identical to those given in Table 1 for each alcohol.

In our previously published study of cyclooctene epoxidation catalyzed by $(F_{20}TPP)FeCl$ dissolved in methanol/acetonitrile solutions, we reported that both Y_∞ and k_{obs} change in a nonlinear fashion with increasing concentration of methanol.[28] Figure 6 shows these effects for methanol and all of the other alcohols considered in the present study. To explain the dependence of k_{obs} on the concentration of alcohol in the solvent, it is necessary to recognize that K_1 is a function of alcohol concentration. We have recently shown

(38) Goh, Y. M.; Nam, W. *Inorg. Chem.* **1999**, *38*, 914−920.

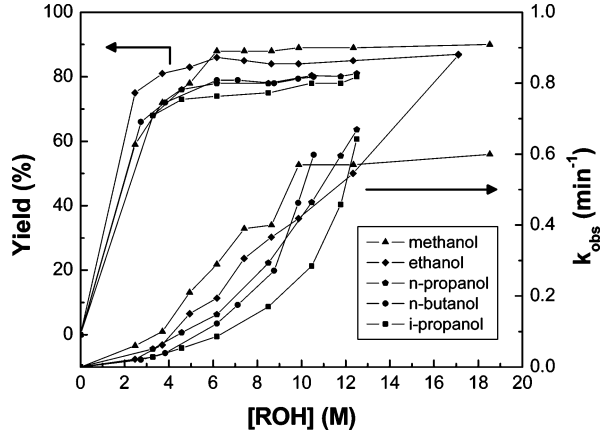

Figure 6. Effects of alcohol concentration on k_{obs} and Y_∞ when the alcohol concentration is varied while keeping the porphyrin concentration fixed at 75 μM. The upper data points correspond to the yield, and the lower data points correspond to the observed rate coefficient.

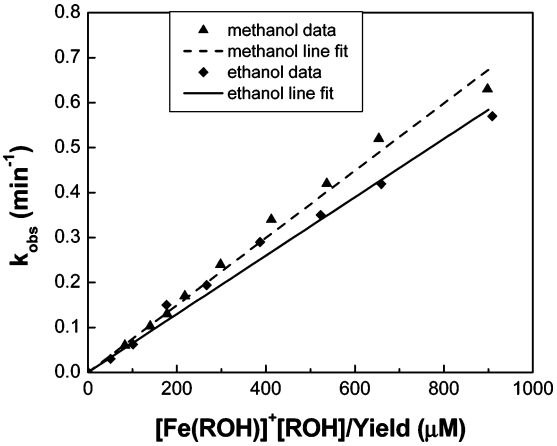

Figure 7. Relationship between k_{obs} and [Fe − ROH][ROH]/Y_∞ when the alcohol concentration is varied while the porphyrin concentration is kept constant at 75 μM.

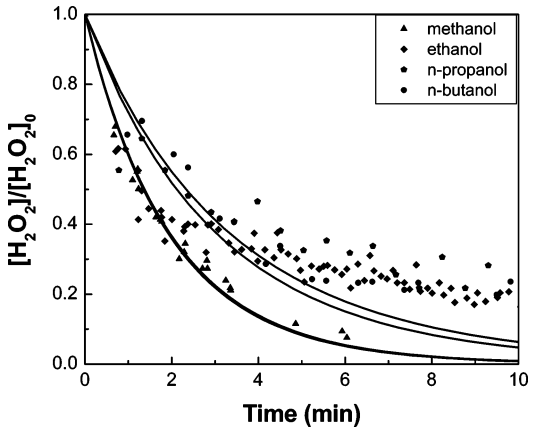

Figure 8. Temporal profiles for H_2O_2 decomposition in the absence of cyclooctene. The solid lines represent the H_2O_2 concentration as predicted from theory, and the data points represent the H_2O_2 concentration as measured by ^{1}H NMR.

that this dependence arises from the fact that the enthalpy of dissociation of (F_{20}TPP)FeCl is linearly dependent on the concentration of alcohol; thus, K_1 can be described by

$$K_1 = K_1^0 \exp[-(\Delta H_0 + \alpha[\mathrm{ROH}])/RT]$$

whereK_1^0 is the pre-exponential factor, ΔH_0 is the enthalpy of dissociation of (F_{20}TPP)FeCl in pure acetonitrile, and α is the dependence of the enthalpy of dissociation on the alcohol concentration.[29] For methanol, the values of ΔH_0 and α are 6 kcal·mol^{-1} and −0.2 kcal·mol^{-1}·M^{-1}, respectively. Therefore, K_1 increases exponentially with increasing methanol concentration. A similar exponential relationship between K_1 and the concentration of ethanol was observed in the course of the present study. Since such measurements require substantial amounts of NMR time,[29] values of ΔH_0 and α were not determined for ethanol, and neither were the dependences of K_1 on alcohol concentration for propanol and butanol. Nevertheless, when the effects of alcohol concentration on K_1 are taken into account and the dependence of k_{obs} on alcohol concentration is determined from eqs 1−3, one obtains the expected relationship of k_{obs} on [Fe − ROH][ROH]/Y_∞. As shown in Figure 7, the dependence of k_{obs} on [Fe − ROH][ROH]/Y_∞ is linear for both methanol and ethanol solutions for a fixed concentration of (F_{20}TPP)FeCl. Moreover, the value of k_3K_2 determined from the slope of the straight line for each alcohol is equivalent to that listed in Table 1, which was obtained for a single alcohol concentration of 6.2 M.

Peroxide Decomposition in the Absence of Substrate. In our studies using methanol/acetonitrile mixtures as the solvent, we observed that the kinetics of H_2O_2 decomposition in the absence of cyclooctene could be described very accurately using the same rate parameters as those used to describe the epoxidation of cyclooctene.[28] The question then is whether the same is true when other alcohols are used instead of methanol. Figure 8 shows the experimental data for the fractional decomposition of H_2O_2 as a function of time for different alcohol/acetonitrile mixtures. The solid curves represent the concentration profiles calculated using the rate parameters given in Table 1 (Note: the curves for methanol and ethanol overlap). While the theoretical curves are consistent with the data in all cases down to $[H_2O_2]/[H_2O_2]_0 \approx 0.3$, the experimentally observed rate of decomposition slows down substantially for long reaction times. The only exception is for methanol. The deviation between experiment and theory is particularly noticeable when the cosolvent is ethanol, but is also pronounced for propanol and butanol. Another interesting observable is difference in the UV−visible spectra taken for H_2O_2 decomposition in methanol/acetonitrile and ethanol/acetonitrile. These results are shown in Figure 9. As was shown previously,[28] when the reaction is carried out in a solution containing methanol, the peak near 390 nm, which is attributed to [(F_{20}TPP)Fe(CH_3OH)]$^+$, decreases at the same time that the peaks at 410 and 540 nm, which are characteristic of Fe(IV) porphyrin species, grow. After a few minutes, though, the spectrum reaches a steady state and then no longer changes in shape. The slow loss of overall intensity is due to porphyrin degradation (see below). On the other hand, when the reaction is carried out in the presence of ethanol, the band at 390 nm declines monotonically and the band at 540 nm grows monotonically. Thus, in an ethanol-containing solu-

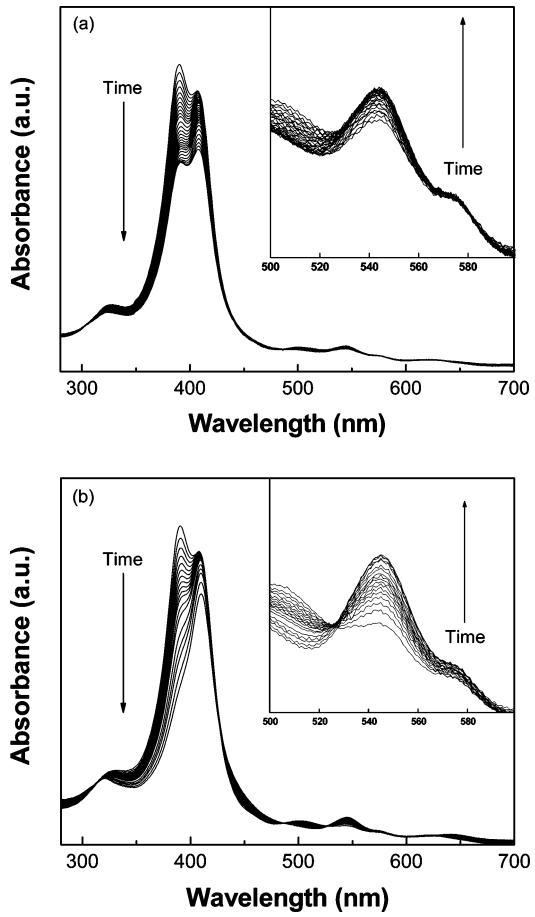

Figure 9. UV−visible spectra taken as a function of time during the decomposition of hydrogen peroxide in the absence of cyclooctene: (a) in a methanol/acetonitrile solvent system and (b) in an ethanol/acetonitrile solvent system. For these experiments, the concentrations of porphyrin and hydrogen peroxide were one-fifth of those used for other kinetic studies (see Table 1). The concentration of alcohol for both experiments was 6.2 M.

tion, Fe(III) species are consumed continuously and Fe(IV) species are produced continuously, and in contrast to methanol-containing solutions, a steady-state balance between these two species is never reached.

The trend in the relative concentrations of Fe(III) and Fe(IV) porphyrin species observed in Figure 9b for ethanol-containing solutions can be rationalized by assuming that the following elementary process, Reaction 8, occurs

$$[(F_{20}TPP)Fe^{III}(ROH)]^+ + HO^\bullet \rightarrow [(F_{20}TPP)Fe^{IV}(OH)(ROH)]^+$$

The effect of Reaction 8 is to reduce the concentration of $[(F_{20}TPP)Fe(ROH)]^+$ cations that can participate in Reaction 2. At the onset of H_2O_2 decomposition, the concentration of $HO^\bullet$ radicals will be small, but as the reaction proceeds, the concentration of these radicals builds up. It can be shown that the slower the rate of H_2O_2 decomposition, the higher will be the concentration of $HO^\bullet$ radicals in solution at a given time, and hence the faster will be the rate of Reaction 8. As discussed above, the rate of Reaction 3 decreases with increasing length of the alkyl chain in the alcohol, i.e., k_3K_2 decreases. Since Reactions 3 and 6 proceed at equal rates, a reduction in the rate of Reaction 3 results in a net decrease in the rate of H_2O_2 consumption and hence to a rise in the concentration of $HO^\bullet$ radicals at a given reaction time. Furthermore, reducing the rate of heterolytic cleavage by either reducing the concentration of alcohol or by increasing the length of the alcohol alkyl chain results in a decrease in the observed rate constant, an increase in the rate of homolytic cleavage relative to the rate of heterolytic cleavage, and a consequent increase in the concentration of $HO^\bullet$ radicals present at a given reaction time. A steady-state balance on Fe(III) and Fe(IV) species can be maintained only until the concentration of $HO^\bullet$ radicals becomes so large that the inclusion of Reaction 8 leads to a continual build up in the concentration of Fe(IV) and a corresponding decrease in the concentration of Fe(III) species. When this occurs, the rate of H_2O_2 decomposition decreases relative to that occurring prior to the build up of $HO^\bullet$ radicals; this effect is what is seen in Figure 8.

Porphyrin Degradation. Free radicals ($HO^\bullet$ or $HOO^\bullet$) are thought to be responsible for porphyrin degradation.[22,28] We have shown previously that porphyrin degradation increases as the observed rate constant decreases or as the concentration of radicals in solution increases.[28] As explained above, the concentration of radicals in solution at a given time is expected to increase as the alkyl chain length of the alcohol increases and the observed rate of reaction slows. More importantly, however, the concentration of $HO^\bullet$ radicals increases as the alkyl chain length of the alcohol increases, as a consequence of the decrease in the rate of heterolytic cleavage relative to the rate of homolytic cleavage (i.e., k_3/k_4). The net result of these changes is additional porphyrin degradation, as shown in Table 1. The susceptibility of a porphyrin to degradation increases as the porphyrin or the ligand coordinated to the Fe cation becomes more electron-rich.[1,4−6] The electron-donating ability of alcohol ligands increases with chain length, and hence, this could also contribute to the increased degree of porphyrin degradation observed with increasing alkyl chain length.

Conclusions

It has been shown that $(F_{20}TPP)FeCl$ is catalytically inactive for the epoxidation of cyclooctene by H_2O_2 when dissolved in acetonitrile solution but becomes increasingly active upon the addition of an alcohol to the solvent. Catalyst activation is attributed to the dissociation of $(F_{20}TPP)FeCl$ into cations and anions. Alcohols enhance the extent of dissociation by coordinating to the $[(F_{20}TPP)Fe]^+$ cations and by solvating both the alcohol-coordinated cation and the chloride anion. The equilibrium constant for $(F_{20}TPP)FeCl$ dissociation, K_1, increases with increasing alkyl chain length for normal alcohols, as a consequence of increasing electron density on the O atom of the alcohol. The kinetics of cyclooctene epoxidation and the consumption of H_2O_2 are well described by the mechanism shown in Figure 1. Reaction is initiated by coordination of H_2O_2 to $[(F_{20}TPP)Fe(ROH)]^+$ cations. The O−O bond of the peroxide then cleaves either heterolytically or homolytically. Heterolytic cleavage is facilitated by alcohol (see Figure 2) and occurs

more rapidly the higher the acidity of the alcohol, whereas homolytic cleavage is independent of alcohol composition. Heterolytic cleavage produces Fe(IV) π-radical cations, which are active for the epoxidation of cyclooctene, whereas homolytic cleavage produces Fe(IV) hydroxo cations, which are active for the decomposition of H_2O_2. The Fe(IV) π-radical cations can also be converted to Fe(IV) hydroxo cations by reaction with H_2O_2. The mechanism shown in Figure 1 correctly predicts the dependence of the observed rate coefficient, k_{obs}, and the yield, Y_∞, on the concentrations of H_2O_2, porphyrin, and alcohol for different alcohol compositions.

Acknowledgment. This work was supported by the Director, Office of Basic Energy Sciences, Chemical Sciences Division of the U.S. Department of Energy under Contract No. DE-AC02-05CH11231.

IC0521776